A High Port-Count Wavelength-Selective Switch Using a Large Scan-Angle, High Fill-Factor, Two-Axis MEMS Scanner Array

Jui-che Tsai and Ming C. Wu, *Fellow, IEEE*

***Abstract*—We present a high-port-count (scalable to 1×32) wavelength-selective switch (WSS) using a large scan-angle, high fill-factor, two-axis analog micromirror array in conjunction with a densely packed two-dimensional array of fiber collimators. A partially populated (1×9) WSS exhibits a fiber-to-fiber insertion loss of 5.57 ± 1.4 dB and an extinction ratio of 51 ± 11 dB. The channel spacing is 100 GHz.**

***Index Terms*—Microelectromechanical systems (MEMS), two-axis micromirror, wavelength-division multiplexing (WDM), wavelength-selective switch (WSS).**

I. Introduction

MICROELECTROMECHANICAL systems (MEMS)-based wavelength-selective switches (WSSs) have drawn a great deal of attention as they enable management of optical networks at wavelength level [1]–[10]. They are also the building blocks of wavelength-selective crossconnets [1]. The use of MEMS technologies provides low optical insertion loss and crosstalk, independence of polarization and wavelength, as well as optical transparency for bit rate and data format. Generally, free-space optical MEMS systems [1]–[8] and hybrid planar lightwave circuit (PLC)-MEMS systems [9], [10] are the two major architectures to implement MEMS-based WSSs. Until now, free-space $1 \times N$ WSSs realized by one-axis micromirror arrays have a port count of $N = 4$, limited by optical diffraction [1]–[3]. WSS with larger port count ($N \geq 8$) is desirable for wavelength-division-multiplexing (WDM) networks. Such a high port-count WSS can be achieved by combining a two-dimensional (2-D) collimator array with a two-axis beamsteering mechanism for each wavelength [4]–[8]. We call this architecture $1 \times N^2$ WSS [4]–[8]. Previously, we demonstrated a free-space $1 \times N^2$ WSS using a monolithic two-axis analog micromirror array with crossbar torsion springs and terraced electrodes [5], [6]. However, the micromirror array available for the system had relatively small scan angles ($\pm 2.63^\circ$ and $\pm 1.27^\circ$ mechanical angles in the x and y directions, respectively), which only covered a 3×5 collimator array [5].

Manuscript received February 22, 2006; revised April 13, 2006. This work was supported by the Defense Advanced Research Projects Agency (DARPA)/SPAWAR under Contract N66001-00-C-8088, by National Taiwan University, Taiwan, and by the National Science Council (NSC) of Taiwan under Contract NSC 94-2218-E-002-082.

J.-C. Tsai is with the Graduate Institute of Electro-Optical Engineering and the Department of Electrical Engineering, National Taiwan University, Taipei 106-17, Taiwan, R.O.C. (e-mail: jctsai@cc.ee.ntu.edu.tw).

M. C. Wu is with the Department of Electrical Engineering and Computer Sciences and Berkeley Sensor and Actuator Center (BSAC), University of California at Berkeley, Berkeley, CA 94720-1774 USA.

Digital Object Identifier 10.1109/LPT.2006.877235

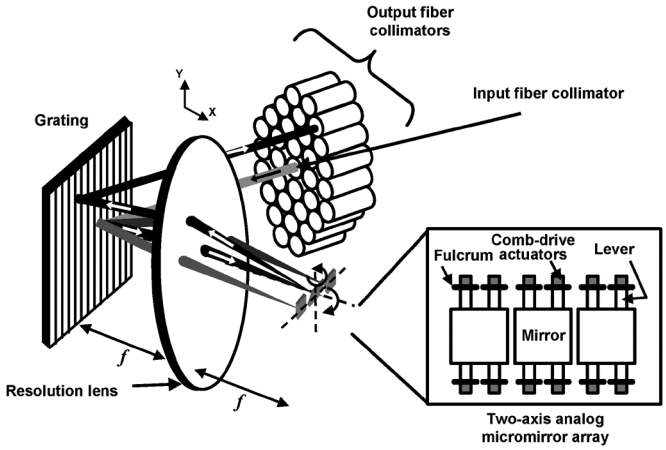

Fig. 1. Schematic of the $1 \times N^2$ WSS using a two-axis analog micromirror array and a densely packed 2-D collimator array. The inset shows the schematic of the MEMS micromirror array.

A 1×9 WSS has been reported using the hybrid PLC-MEMS approach. Two PLC chips, each with five input/output ports, are stacked vertically [10]. This architecture is analogous to the free-space $1 \times N^2$ WSS and also requires a two-axis micromirror array.

Recently, we reported the preliminary results of a free-space $1 \times N^2$ WSS using a new micromirror array with significantly larger scan angles ($\pm 6.7^\circ$ mechanically for both axes) [8]. In this letter, we present the details of the WSS using such two-axis mirrors. By using a tightly packed collimator array (see Fig. 1), a 1×32 (1×9 partially populated) WSS can be achieved.

II. $1 \times N^2$ WSS

Fig. 1 shows the schematic of the $1 \times N^2$ WSS with a two-axis micromirror array and a 2-D collimator array. The collimated optical beam carrying the WDM signals is spatially dispersed by a diffraction grating. Each wavelength channel is then focused onto its corresponding micromirror by a resolution lens. The two-axis MEMS scanners steer individual wavelengths to any arbitrary output port in the 2-D collimator array, depending on the mirror scanning directions and angles.

Currently, discrete collimators are used to simulate the 2-D collimator array in our experiment. The focal length of the 2-in resolution lens is 150 mm, and an 1100-grooves/mm grating is used.

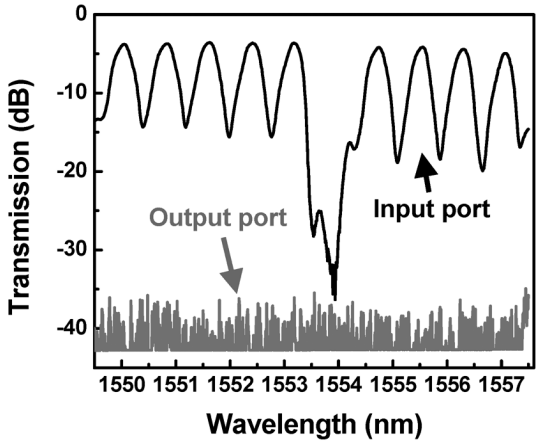

(a)

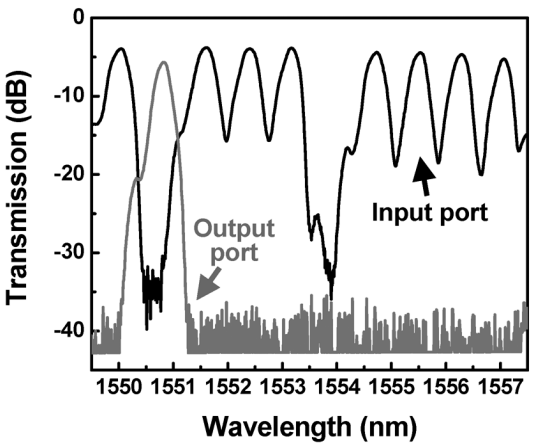

(b)

Fig. 2. Spectral responses at the input and output fibers when (a) all the channels are coupled back to the input port, and (b) the 1550.8-nm channel is switched to the output port (0.5, 2). The dip at 1554 nm is due to a mirror experiencing snap-down during testing.

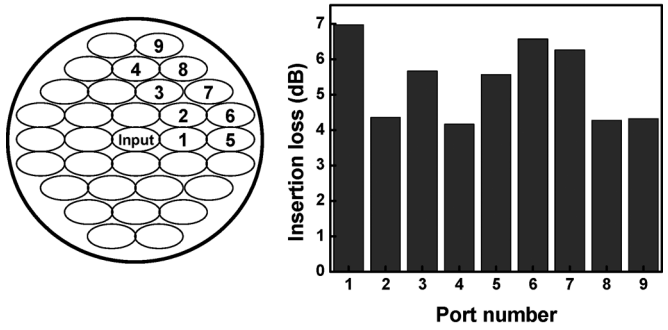

(a)

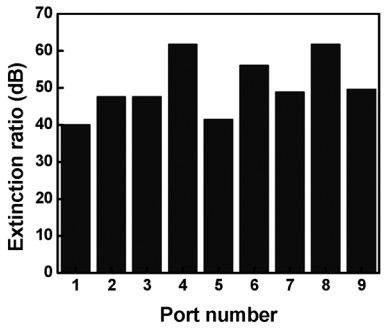

(b)

Fig. 3. Distributions of (a) insertion loss and (b) extinction ratio across the nine populated output ports located in one quadrant. The insertion loss is 5.57 ± 1.4 dB while the extinction ratio is 51 ± 11 dB.

The new micromirror used in our optical system employs four lever arms to amplify the scan angle in both rotation axes. Each lever arm is driven electrostatically by a compact vertical comb-drive actuator. The maximum mechanical scan angle achieved is $\pm 6.7^\circ$ at 75 V for both axes [7]. The scan angle in the diagonal direction is slightly smaller $(\pm 4.7^\circ)$ due to the longer mirror length. The area of the micromirror is $196 \times 196\ \mu\text{m}^2$, on a 200-$\mu$m pitch. The resonant frequency of the mirror is 5.9 kHz before metallization. The array size of the MEMS mirrors is 1×10 (ten wavelength channels), which is restricted by the available area of the current chip $(3 \times 6\ \text{mm}^2)$.

33 discrete collimators can be covered by the lens area and mirror scan angles (see Fig. 1). The central collimator is used as the input port. This minimizes the required mirror scan angle for reaching every port in the collimator array. The resulting port count of the current system is 1×32 (1×9 partially populated).

III. System Performance

The spectral responses of various switching states are measured. Fig. 2(a) shows the spectra when all ten wavelengths are coupled back to the input port. The signal is measured through a circulator at the input port. Very uniform loss is observed across the ten wavelength channels. If we label the collimators by Cartesian coordinates with the input port located at the origin, (0, 0), the output port measured here is situated at (0.5, 2) position (i.e., Port 3 in Fig. 3). Note that the collimators are not arranged in a square array to achieve higher packing density (see Fig. 1). The dip at 1554 nm is due to a mirror experiencing snap-down during testing. (The MEMS mirrors used in this experiment are not packaged.) Fig. 2(b) shows the spectra when the 1550.8-nm channel is switched to the output port.

The distribution of fiber-to-fiber insertion loss across the nine populated output ports is 5.57 ± 1.4 dB [Fig. 3(a)]. When coupled back to the input port, the insertion loss is 3.72 dB. The port-dependent loss may be a consequence of system misalignment, lens aberrations, or grating image position dependence on output port. The extinction ratio within the same set of outputs is measured to be 51 ± 11 dB [Fig. 3(b)]. The shape of the collimator images in Fig. 3 is elliptical due to the anamorphic effect caused by the diffraction grating. The extinction ratio of the input port is 30 dB for the switched channel (see Fig. 2), which matches well with calculated value for the current mirror size. It can be further increased by extending the mirror size in the vertical direction. The spacing between collimator centers ensures crosstalk of < -40 dB from an adjacent port. The grating efficiency depends strongly on the light polarization. The S-polarization exhibits much higher diffraction efficiency than the P-polarization, which leads to a polarization-dependent loss (PDL) of approximately 24 dB in the system. This relatively high PDL may be significantly suppressed by employing polarization diversity optics [3].

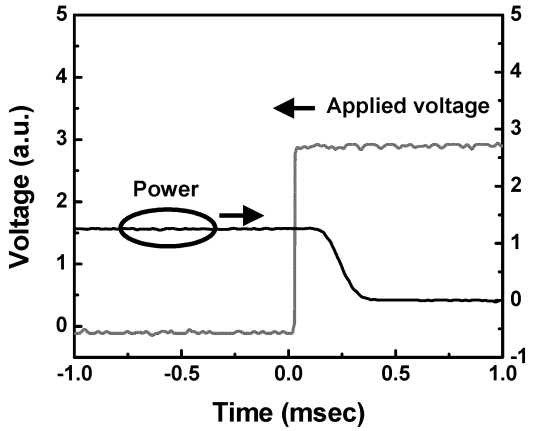

Fig. 4. Dynamic switching response.

The channel spacing of the WSS is 100 GHz. The measured width of the passband is narrower than that expected for our mirror size. This is attributed to the MEMS mirror curvature ($\sim$8 mm) induced by the metal coating. The measured passband width matches well with the simulation using this mirror curvature. Simulation also shows that the 1-dB passband width can be improved to 75 GHz with a radius of curvature of 20 mm.

Fig. 4 is the temporal response at the input port during switching. A square wave is applied on the mirror. The switching time is less than 0.5 ms.

IV. Conclusion

We have demonstrated a high-port-count WSS capable of scaling to 1×32 using a large scan-angle, two-axis MEMS scanner array. The high port count is enabled by the large scan range of the two-axis micromirror array ($\pm 6.7^{\circ}$ mechanically in both axes). Our bench top experimental prototype with 1×9 ports exhibits an optical insertion loss of 5.57 ± 1.4 dB, and an extinction ratio distribution of 51 ± 11 dB. The channel spacing is 100 GHz.

Acknowledgment

The authors would like to thank L. Fan, D. Hah, M.-C. Lee, C.-H. Chi, W. Piyawattanametha, and S.-T. Hsu for discussions and assistance.

References

[1] T. Ducellier *et al.*, "The MWS 1×4: A high performance wavelength switching building block," in *Proc. Eur. Conf. Optical Communication (ECOC 2002)*, Copenhagen, Denmark, Session 2.3.1.

[2] J. C. Tsai, S. Huang, D. Hah, H. Toshiyoshi, and M. C. Wu, "Open-loop operation of MEMS-based $1 \times N$ wavelength-selective switch with long-term stability and repeatability," *IEEE Photon. Technol. Lett.*, vol. 16, no. 4, pp. 1041–1043, Apr. 2004.

[3] D. M. Marom *et al.*, "Wavelength-selective $1 \times K$ switches using free-space optics and MEMS micromirrors: theory, design, and implementation," *J. Lightw. Technol.*, vol. 23, no. 4, pp. 1620–1630, Apr. 2005.

[4] J. C. Tsai, S. Huang, D. Hah, and M. C. Wu, "$1 \times N^2$ wavelength-selective switch with two cross-scanning one-axis analog micromirror arrays in a $4 - f$ optical system," *J. Lightw. Technol.*, vol. 24, no. 2, pp. 897–903, Feb. 2006.

[5] J. C. Tsai, S. Huang, and M. C. Wu, "High fill-factor two-axis analog micromirror array for $1 \times N^2$ wavelength-selective switches," in *Proc. MEMS 2004*, pp. 101–104.

[6] J. C. Tsai and M. C. Wu, "Gimbal-less MEMS two-axis optical scanner array with high fill-factor," *J. Microelectromech. Syst.*, vol. 14, no. 6, pp. 1323–1328, Dec. 2005.

[7] J. C. Tsai, L. Fan, D. Hah, and M. C. Wu, "A high fill-factor, large scan-angle, two-axis analog micromirror array driven by leverage mechanism," in *Proc. 2004 IEEE/LEOS Optical MEMS Conf.*, pp. 30–31.

[8] J. C. Tsai, L. Fan, C. H. Chi, D. Hah, and M. C. Wu, "A large port-count 1×32 wavelength-selective switch using a large scan-angle, high fill-factor, two-axis analog micromirror array," in *Proc. Eur. Conf. Optical Communication (ECOC 2004)*, Stockholm, Sweden, Paper Tu1.5.2.

[9] D. M. Marom *et al.*, "Wavelength-selective 1×2 switch utilizing a planar lightwave circuit stack and a MEMS micromirror array," in *Proc. 2004 IEEE/LEOS Optical MEMS Conf.*, pp. 28–29.

[10] T. Ducellier *et al.*, "Novel high performance hybrid waveguide-MEMS 1×9 wavelength selective switch in a 32-cascade loop experiment," in *Proc. Eur. Conf. Optical Communication (ECOC 2004)*, Stockholm, Sweden, Paper Th4.2.2.